A model for the electrical conductivity variation of molten polymer filled with carbon nanotubes under extensional deformation

Marjorie Marcourt, Philippe Cassagnau, René Fulchiron, Dimitri Rousseaux, Olivier Lhost, Simon Karam

A model for the electrical conductivity variation of molten polymer filled with carbon nanotubes under extensional deformation

Marjorie Marcourt,[†] Philippe Cassagnau,[†] René Fulchiron,*[,†]

Dimitri Rousseaux,[‡] Olivier Lhost,[‡] Simon Karam[‡]

[†]Univ Lyon, Université Claude Bernard Lyon 1, CNRS UMR 5223, Ingénierie des Matériaux Polymères, F-69622, Villeurbanne Cedex, France

[‡]Total Research and Technology Feluy Zone Industrielle Feluy C 7181 Feluy, Belgium

***Corresponding author: rene.fulchiron@univ-lyon1.fr**

Abstract:

This work is dedicated to analyzing the variation of conductivity of polymer composites (polystyrene filled with Carbon Nanotubes) under extensional deformation. In a previous work, a conductor-insulator transition has been observed and the predominant role of the polymer dynamics has been brought to light. The evolution of the filler network within a polymer matrix can be described by a kinetic equation that takes into account a structuring mechanism that is controlled by the mobility in the melt matrix and a destruction mechanism that is induced by the extensional deformation. The solution of this equation that describes the filler network at a microscale is used in the percolation law to obtain the macroscopic conductivity of the composite. It turned out that the structuring parameter does not depend on the extensional deformation but only relies on the polymer matrix dynamics. In addition, the breaking parameter only depends on the Hencky strain, whatever the extensional rate. This model has been successfully applied for a large range of filler concentrations and experimental conditions from low to large Weissenberg numbers.

Keywords: Nanocomposites; Carbon Nanotubes, Extensional Viscoelasticity; Electrical conductivity; Modeling.

1. Introduction

The addition of Carbon Nanotubes is a promising solution for the achievement of Conductive Polymer Composites (CPC). Owing to their large aspect ratio, only a small amount of fillers can turn an insulating polymer matrix to a composite with moderate electrical properties [1-3]. The preferred and reliable method for the filler incorporation is the melt mixing and more precisely the masterbatch dilution that can lead to suitable filler dispersion and distribution within the matrix [4]. Leaving apart all the parameters that must be taken into account (mixing duration, shear rates, filler functionalization) the generation of CPC with suitable electrical properties relies on the formation of a homogeneous network made of small aggregates, disentangled amounts of CNTs and individual CNTs [5-7].

The use of rheological analysis combined with conductivity monitoring has paved the way for the comprehension of the filler network behavior in molten composites under both quiescent and small shear strain [8]. Indeed, the “dynamic percolation” [5,9-13] and the conductor/insulator transition [14,15] have been brought to light. Those two specific mechanisms illustrate the huge capacity of the filler structure to evolve. The network build-up has been explained by Alig *et al*. [5] as the combination between strong dispersive interactions between nanotubes and depletion interactions between the diffusion of isolated CNTs that is made possible if the polymer viscosity is sufficiently low. The network destruction is more complex and is intimately linked to the filler network structure. In fact, it has been observed that under shear deformation at large shear rates [16] or under extensional deformation [17], the agglomerates are stretched and orient in the deformation direction. The aggregates network morphology changes in response to strains and, more precisely, its response is linked to its initial morphology [15,18,19]. Similarly to highly filled materials whose flow behavior depends on the filler network structure, the electrical

properties of CPC are also intimately linked to the filler network structure. The structural evolution of highly filled material has been widely investigated and is well described by a kinetic equation introduced by Barnes [20] for heterogeneous materials [21-26] as:

$$\frac{d\xi}{dt} = a(1-\xi)^b + c\xi\dot{\gamma}^d \qquad \textbf{Equation 1}$$

where ξ is a structural parameter that describes the filler agglomeration state: ξ = 1 the agglomeration state in the network is maximum and entirely efficient and ξ = 0 the network is fully broken. The constants *a*, *b*, *c* and *d* are linked to the material. The first term describes the network reinforcement and the second depending on the sign of *c* illustrates the shear-induced agglomeration or the shear-induced destruction. For instance, Leonov *et al.* [26] argued that the breakup depends on the second invariant of the rate of deformation $II_{\dot{\gamma}}$.

The conductivity variation due to the CNT network evolution has been first described by Alig *et al*. [5,14]. They combined a kinetic equation which takes into account the evolution of the agglomerates fraction contributing to the conduction (φ_{eff}), with a percolation law to associate the network structure to the electrical properties of the composite.

$$\frac{d\varphi_{eff}}{dt} = k_0(\varphi - \varphi_{eff})^n + k_1\left(\varphi - \varphi_{eff}\right) - k_2\varphi_{eff} \qquad \textbf{Equation 2}$$

where φ is the filler total fraction, considering that, at equilibrium (when $t \to \infty$) all the CNTs contribute to the conductive network, φ_{eff} is the volume fraction of conductive agglomerates k_0, k_1 and k_2 are the kinetic coefficients for respectively quiescent agglomeration, shear-stimulated agglomeration and shear-stimulated destruction process.

It must be noticed that k_1 and k_2 depend on the shear rate $\dot{\gamma}$. Alig *et al*. argued first that the network building was a second order mechanism (*n*=2) considering the agglomeration process as a clustering mechanism where two non-conductive particles stick together to create an electrically conductor agglomerate. Later, Skipa and coworkers [18,19] have shown that the value of *n* equal to 1 leads also to relevant results. Then, the solution of the kinetic

equation is introduced into the percolation law that describes the macroscopic behavior of the composite. This model well describes the different conductivity evolutions observed under shear deformation at small shear rates. For instance, it can describe the interplay between build-up and destruction when the conductivity curve merges to a steady value [2,19]. The evolution of k_0 remained unexplained even if the authors highlighted the influence of the temperature on the conductivity recovery. In addition, Alig and coworkers [27] have observed large difference between the reaction rate k_0 for conductivity recovery experiments of comparable specimens. Surprisingly, for a shear-induced agglomeration that led to an increase of conductivity greater than six decades, they observed that the sum of the structuring parameter was very close to the breaking parameter. Moreover, they have proposed a destruction rate that depends on the shear rate (see Equation 2) [18,19] but did not deduce an obvious relation from the fitted parameters.

In this paper, a new approach to describe the destruction mechanism, especially for extensional strain, will be introduced and applied to the composites on the basis of conductivity measurements during extensional deformation.

2. Material and Methods

The CNTs are the NC7000 supplied by Nanocyl, a Belgian company. They are characterized by a diameter *d* around 9.5 nm and a mean length of 1.5 µm. The matrix used is a polystyrene (PS) with a melt flow index of 2.4 supplied by Total. The composites were melt mixed using a masterbatch dilution strategy and were supplied by Total as pellets. The concentration of CNTs in the initial masterbatch was of 15wt%. It was then dry blended with pure PS to reach the desired filler concentration before extrusion. From the supplied pellets, the specimens were compression molded at 200°C. A pressure of 20 bars was applied to the

mold for 10 minutes. Then, the pressure was increased to 200 bars in 10 minutes and held during 5 min. Then, the specimen was cooled down to room temperature.

Electrical properties analysis has been conducted on compression molded samples that have been additionally submitted to a quiescent treatment at 200°C for around 20 min. This supplementary thermal treatment enables the filler network to recover an equilibrium state in which most of the CNTs take part to the electrical conduction. Indeed, just after the compression molding, this state is not obtained. The good contact between the electrodes and the specimen was ensured using a colloidal silver paste. Owing to a Keithley 237 power supply, a 10 volt Direct Current (DC) is delivered and the current passing through the sample is measured. The volume conductivity is then deduced using the specimen geometry as:

$$\sigma = \frac{L.I}{S.U} \qquad \textbf{Equation 3}$$

with U the applied voltage, I the measured current, L and S respectively the specimen length and section. From these experiments, the percolation law linking the conductivity to the effective CNT's fraction was determined on specimens that have been annealed [17]:

$$\sigma = \sigma_0(\varphi_{eff} - \varphi_c)^{\beta} \qquad \textbf{Equation 4}$$

with φ_{eff} ($\geq \varphi_c$), the effective volume fraction of CNTs which contribute to the conduction and φ_c the percolation threshold. It must be added that, since the samples have been annealed, the efficient fraction (φ_{eff}) of CNTs has been e assimilated to the total fraction (φ) to determine the parameters of this law. The obtained exponent β is 2.2 with a percolation threshold φ_c at 0.19 vol% and a pre-factor σ_0 of 630 S.cm^{-1}.

Extensional experiments were carried out with a Extensional Viscosity Fixture EVF (TA Instruments) mounted on the ARES rheometer (TA Instruments). The set-up was modified in order to measure the specimen conductivity during the extensional test. This specific set-up has already been detailed in an earlier work [17]. In some cases, the measurements have

been carried out on samples directly after their compression molding without the annealing treatment. By this way, the structuring mechanism is not fully accomplished at the beginning of the experiment so that it can be caught during the measurements.

The differential equations which do not have an analytical solution were numerically resolved using the software Scilab (open source software published by Scilab Enterprises S.A.S). All the fitted parameters presented in this work were obtained by the means of a non-linear least squares regression method.

3. Description of the proposed model

3.1. Network structuring

The CNT network is made of aggregates that are connected together by individual CNTs or highly disentangled group of CNTs that constitute junctions between aggregates. Thermal diffusion triggers the formation of junctions and hence the filler network reinforcement [17]. The structuring rate depends on the difference from the equilibrium state in a manner analogous to the model of Skipa *et al.* Even if we have been very cautious of the specimen's preparation, it remains possible that the initial state can slightly vary. The difference will be observed for specific specimens and will be detailed later in this work. The effective filler fraction that takes part to the conductivity is considered as the structural variable. Hence, the network structuring kinetics is given by:

$$\left.\frac{d\varphi_{eff}}{dt}\right|_{structuring} = k_{build}(\varphi - \varphi_{eff}) \qquad \textbf{Equation 5}$$

where φ_{eff} is the filler that belongs to the percolated network; φ is the total filler concentration in the specimen and consequently, the upper limit of φ_{eff}. It can be pointed out that ξ appearing in Equation 1 would be φ_{eff}/φ in our notation. The parameter k_{build} has the dimension of the inverse time. The aggregation and the formation of connections can only be disrupted by deformation. Indeed, the theoretical energy required to counter

the strong attractive forces between CNTs is around $1000k_BT$ (T is the temperature and k_B is the Boltzmann's constant) [28]. The structuring mechanism is pretty complex and embraces different mechanism at different scale but for states relatively close to the equilibrium, Equation 5 is acceptable. The filler network can be seen as a 3D structure made of CNTs. All the CNTs can be considered as equivalent sites for the binding of isolated CNTs or small aggregates. It can be added that, taken alone, Equation 5 has an analytical solution which asymptotically tends to φ.

$$\varphi_{eff} = \varphi + (\varphi_0 - \varphi)\exp(-k_{build}t) \qquad \textbf{Equation 6}$$

where φ_0 is the initial effective filler concentration which is different from φ when the material is not initially at equilibrium.

3.2. Network breakup

In our previous work, from Scanning Electron Microscopy, it has been shown that the aggregates and CNTs of an initially isotropic filler network orientate under extensional deformation [17]. Thus, it can be considered that, the network is first stretched and then, the CNTs are strained apart from each other as shown in Figure 1.

Figure 1: Evolution of the filler network under extensional deformation

The first step does not induce major conductivity evolution as the orientation does not or very slightly impact of connections within the network [29,30]. Thus, it can be assumed that extensional strains do not induce any increase of the number of connections. Depending on the experimental conditions, this stage can take more or less time. However, when the CNTs are fully extended, the deformation will progressively pull apart the CNTs

and the aggregates from each other. The number of connections will progressively decrease and so will the conductivity.

In Figure 1, the number of connections that are represented by the grey circles does not vary in early stage but dramatically decreases when the CNTs are fully extended. In that sense, it will be considered that the filler network is broken for a given limiting Hencky strain and that it is still efficient for a strain lower than this limit. From a mathematical viewpoint and avoiding any discontinuity which could provide numerical difficulties, the network breakup can be expressed using a simple decreasing sigmoid:

$$\varphi_{eff} = \varphi e^{-(k_{break}\varepsilon^2)} \qquad \textbf{Equation 7}$$

where k_{break} is the adimensional breaking parameter. It can be pointed that the exponent of the strain in Equation 7 could have been left as an adjustable parameter. However, the suitability of the value of 2 will be shown further.

For extensional measurements, where $\varepsilon = \dot{\varepsilon}t$, the time derivative of equation 7 leads to

$$\left.\frac{d\varphi_{eff}}{dt}\right|_{destruction} = -2k_{break}\dot{\varepsilon}^2\,\varphi_{eff}t \qquad \textbf{Equation 8}$$

It can be added that, a priori, the breaking parameter k_{break} may be dependent on the extensional rate. This will be discussed further.

As a whole, the evolution of the CNTs that belongs to the percolated network (φ_{eff}) is the sum of the building (Equation 5) and destruction (Equation 8) parts.

$$\frac{d\varphi_{eff}}{dt} = k_{build}\left(\varphi - \varphi_{eff}\right) - 2k_{break}\dot{\varepsilon}^2\,\varphi_{eff}t \qquad \textbf{Equation 9}$$

This differential equation was numerically solved using the Ordinary Differential Equation solver of the software Scilab. The solution of Equation 9 was then inserted into the percolation law (Equation 4) to obtain the conductivity as a function of time.

The initial effective filler concentration φ_0 is also determined by means of the percolation law, simply adjusting φ_0 to calculate the initial conductivity (if the material is not

initially at equilibrium). Then, using a nonlinear least square regression algorithm, the two parameters k_{build} and k_{break} were fitted to the experimental data.

4. Results and Discussion

4.1. Validation of the model for one CNT content

In our previous work [17], we have shown that the conductivity variation of CPC under extensional deformation can be linked to the Weissenberg number expressed as:

$$W_i = \lambda_w . \dot{\varepsilon} \qquad \textbf{Equation 10}$$

where λ_w is the characteristic time taken as the weight average relaxation time of the pure matrix deduced from a *N* modes Maxwell model [31] applied on the master curve of the pure matrix [32]. For low W_i, there is a strong competition between the network restructuring and breakup. However, at large W_i, the destruction is predominant and from this point all the curves merge to the same maximal deformation that is when the specimen become electrically insulating. Without going into details, the choice of the weight average relaxation time among different possible averaging has been guided by the fact that it more reflects the polymer viscoelastic behavior because it contains the effect of both the average molar mass and the molar mass distribution.

Figure 2 shows, on a linear scale, the measured and calculated conductivities for low W_i. First, it can be observed that the proposed model well describes the strong competition between network structuring and breakup that is characterized by the maximum of conductivity in Figure 2. Obviously this type of maximum is present only if the sample is not initially at equilibrium as a consequence of its preparation process ($\varphi_0 < \varphi$). In this respect, it can be mentioned that this effect of a relaxation was already shown [17] by recording the conductivity increase after cessation of elongation. For comparison, the conductivity calculated using the model proposed by Skipa *et al* [18, 19] and applied to extensional strain

is also shown in Figure 2. On this point, it must be recalled that this model has been initially tested only for shearing deformation. However, for extensional deformation, no structuring network induced by the strain has been observed contrary to shear deformation. Indeed, an insulating material will remain insulating under extensional deformation whereas under shear the conductivity can somehow increase [6]. In the present calculation, the parameter k_1' which represents the kinetic factor for the network building is the sum k_0 and k_1 (see Equation 1) and k_2 is the factor governing the network strain-induced breakup.

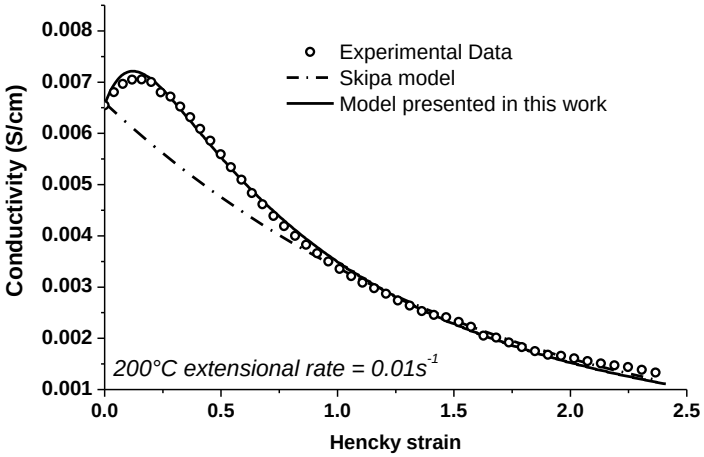

Figure 2: Conductivity variation as a function of the Hencky strain for material PS/MWCNT (0.79 vol%) at 200 °C, 0.01 s^{-1}. Symbols: Experimental data; Semi-dotted line: Curves calculated with the model of Skipa *et al* [18, 19] (best fit with k'_1= 0 s^{-1} and k_2= 0.002 s^{-1}); Solid line: Model of the present work (best fit with k_{build}= 0.084 s^{-1} and k_{break}= 1.5).

Figure 2 shows the model of Skipa *et al.* fails at describing the experimental data. Indeed, the calculated result is inevitably monotonic so that a conductivity growth followed by a decrease cannot be predicted. Moreover, it must be mentioned that, if k_1' had not been imposed to 0, the model prediction would tend to a non-zero steady conductivity value for high deformations contrary to the experiment. It can be added that this conductivity maximum observed in Figure 2 that illustrates the briefly predominance of the building mechanism could have been predicted using the model revision proposed by Skipa *et al.* [19]

where different CNTs populations have been considered (each of them being governed by specific kinetic parameters). However, that would have induced an increase of the adjustable parameters number. Consequently, the authors concluded that the solution of the regression is not unique and it is hard to give a physical meaning to all the set of parameters.

Figure 3 and Figure 4 display the conductivity variation of PS/MWCNT (0.79 vol %) under experimental conditions that comprise low and large W_i values.

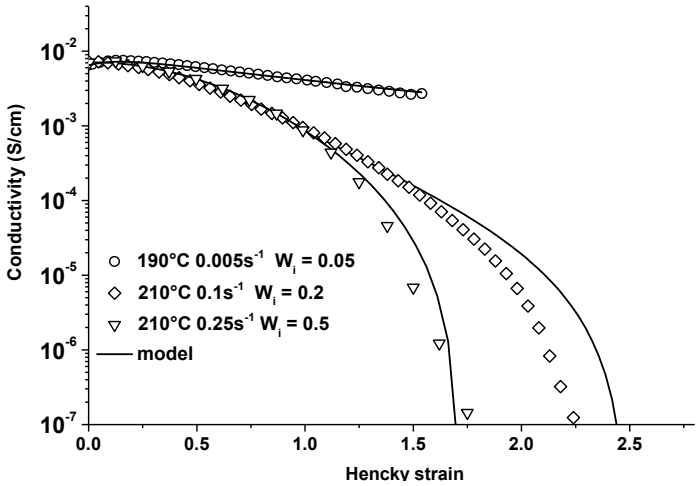

Figure 3: Conductivity as a function of the Hencky strain of PS/MWCNT (0.79 vol%) for low W_i. Symbols: Experimental data; solid lines: Calculated curves.

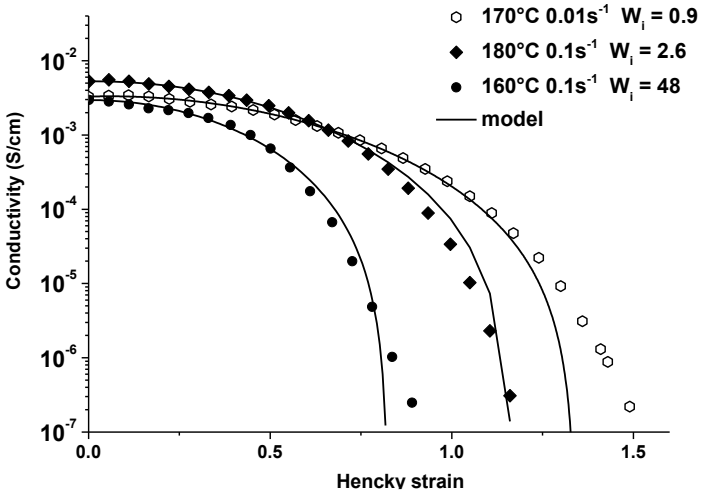

Figure 4: Conductivity as a function of the Hencky strain of PS/MWCT (0.79 vol%) for large W_i. Symbols: Experimental data, solid lines: Calculated curves.

First, the breaking and building parameters have been determined for a large number of experimental data that cover low and medium W_i. In those specific conditions there is a strong competition between network building and breaking so reliable values of k_{build} and k_{break} can be determined. From these calculations, it turned out that the obtained values for the breaking parameter (k_{break}) were practically independent of the temperature and of the extensional rate. This result will be discussed further.

Conversely, for very large W_i, that is for large extensional rates and low temperatures, it was not possible to adjust the structuring parameter because the structuring mechanism was not noticeable in the measured conductivity. In that specific case, only the breaking parameter has been determined. Nevertheless, at moderate and large W_i, (see Figure 4) there is also a good description of the conductivity variation.

Concerning the structuring parameter (k_{build}), an obvious dependence of the obtained values with the temperature was observed whereas they appeared independent of the extensional rate. Moreover, other results that are not detailed in this paper show that this structuring parameter is independent of the filler concentration. This corroborates the assumption that the building mechanism is mainly driven by the polymer mobility in the matrix.

This analysis is summarized in Figure 5 where the variation of the building parameter k_{build} is displayed as a function of the inverse of the weight average relaxation time λ_w. which directly depends on the temperature. The variation of λ_w was deduced from the Williams Landel Ferry equation [32]. The details of the rheological behavior of the used PS matrix are given in Reference [17]. The correlation is very clearly shown in Figure 5 indicating that the building mechanism is controlled by the molecular mobility of the polymer. Indeed, when the viscosity of the polymer decreases, the structuring mechanisms that are composed

of diffusion of single CNTs and agglomeration of close aggregates are enhanced. On the other hand for a frozen polymer ($\lambda_w \to \infty$), the network cannot be rebuilt anymore ($k_{build} \to 0$). Here, a linear dependence between the building parameter and the inverse of the characteristic time of the polymer is obtained. Hence, for the following and for experiments at low temperatures (140°C and 160°C) where the structuring parameter could not be directly fitted on the measured conductivity, it has been calculated from the relation displayed in Figure 5.

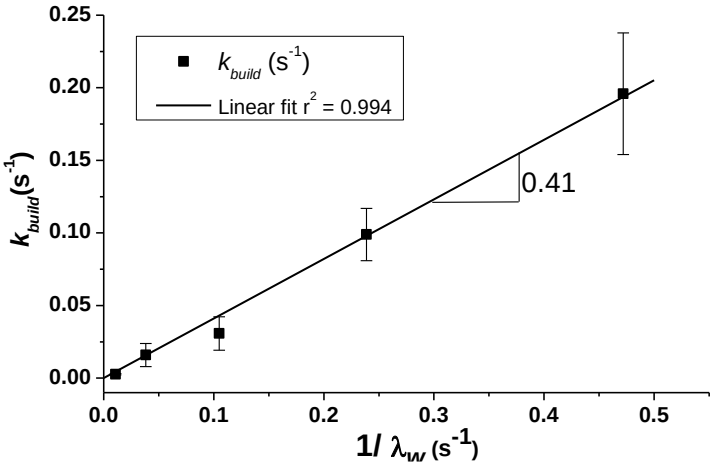

Figure 5: Structuring parameter versus the inverse of the weight average relaxation time of the pure matrix.

This important result shows that the polymer dynamics drives the network structuring. Thus, the building parameter can be obtained from the relaxation time of the pure matrix and the Williams Landel Ferry coefficients for a given temperature. Consequently, Equation 9 can be rewritten:

$$\frac{d\varphi_{eff}}{dt} = \frac{\alpha}{\lambda_{w-T_{ref}} a_T}\left(\varphi - \varphi_{eff}\right) - 2k_{break}\dot{\varepsilon}^2\varphi_{eff}t \qquad \textbf{Equation 11}$$

where α and k_{break} are dimensionless constants that depends on the material (α is characteristic of the matrix and k_{break} characteristic of the filler network).

As regards the breaking parameter k_{break} , the obtained values are summarized in Figure 6 where they are plotted versus the extensional rate. As it was already mentioned, the breaking parameter appears independent of the extensional rate. In this regard, it can be pointed out that this independence is consistent with the approach of Leonov [26] who considered a breaking mechanism dependent on the squared deformation rate as it appears in the second member of Equation 11 (in the model of Leonov, this comes from the second invariant of the shear rate tensor). Then, from all these results, Equation 11 will be used in the following with constant values of α and k_{break}, respectively set to 0.41 and 1.3.

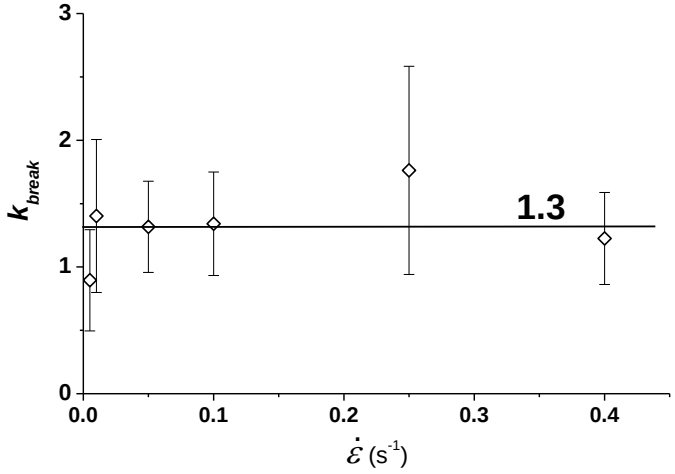

Figure 6: Breaking parameter versus the extensional rate.

4.2. Generalization to other CNT contents

The domain of validity of the model proposed in the present work has been tested on materials with different filler concentrations in the range between 0.38 vol% and 1.9 vol% of CNT in PS and at different extensional rates. Here, for sake of simplification, it is assumed that the filler dispersion quality is comparable for the different tested concentrations. However, it must be conceded that this assumption is questionable especially for large filler concentrations where there is a larger population of big agglomerates and at very low filler concentrations (lower than 0.5vol%) where the fillers are more dispersed and consequently, the structuring mechanism are quite limited.

In a previous work, the Hencky strain where the specimen conductivity reaches 10^{-6} S/cm (ε_σ) has been arbitrarily considered as the transition between conducting and insulating behaviors. This limiting value is again considered here to characterize the composites behavior under different extensional conditions. Figure 7 displays experimental and calculated data obtained at 0.1 s^{-1} and 160, 180, 200 and 210 °C. The experimental data are chosen to cover low and large W_i values. For the calculated data, an initial efficient concentration φ_0 of CNTs that belongs to the percolated network has been set to 95% of the total filler concentration φ. This value corresponds to the initial measured value of conductivity and this illustrates the fact that the specimen is not totally at equilibrium at the beginning of the measurement.

At large W_i, (see Figure 7a and 7b) the model correctly predicts the evolution of ε_σ for different filler concentrations and extensional conditions. Figure 7c and 7d display ε_σ for close W_i values but obtained in different extensional conditions. At W_i = 0.4 there is a very good prediction of the model. However, at W_i = 0.2, the prediction of the model is acceptable, except for large concentrations (higher than 1.2 vol%). In those cases, the maximal deformation is overestimated and even predicts ε_σ that are larger than the specimen deformation at break. Indeed, under extensional deformation, the specimens break approximately after a Hencky strain of 4, however, from a Hencky strain of 3.5, the specimen becomes very thin and the homogeneity of the strain in the sample may not be ensured anymore. Consequently, the structuring mechanism may be disrupted while it is still considered in the model. Hence, at low temperatures, the building parameter is small so that it does not impact the prediction. However, at higher temperature (for instance 210°C) the structuring factor is quite important and leads to an overestimation of the ε_σ.

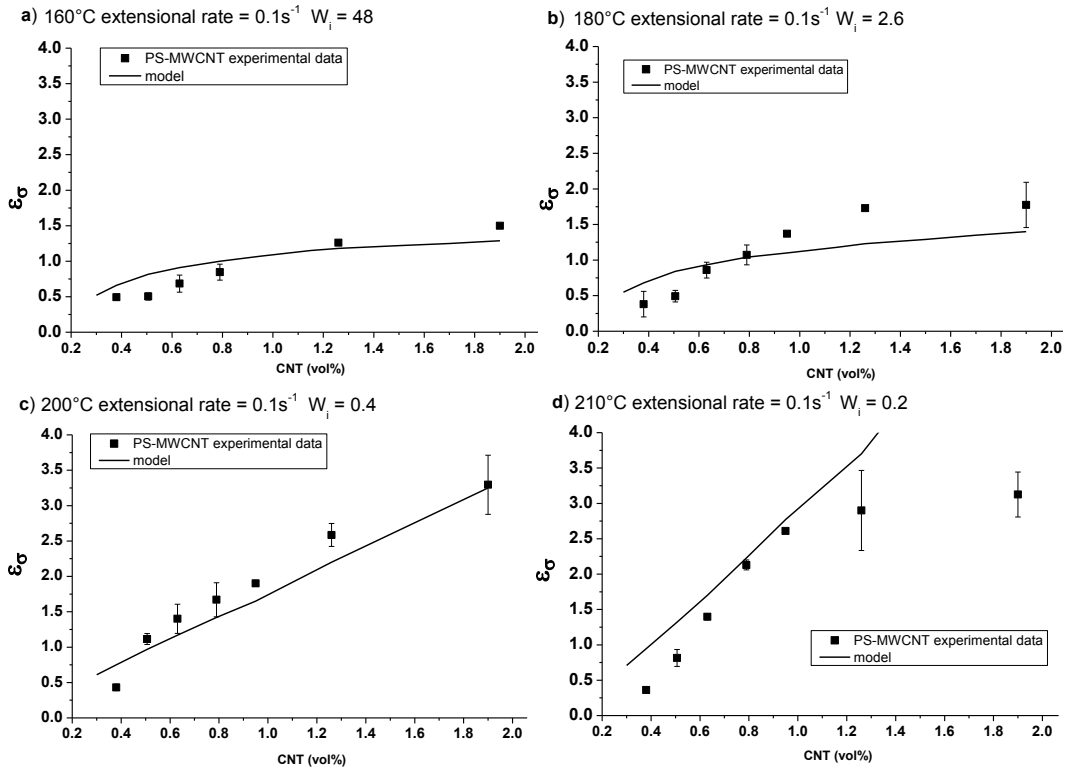

Figure 7: Maximal deformation before conductive/insulating transition for PS filled with CNT (0.37 to 1.9 vol%) for an extensional rate of 0.1 s^{-1} at 160 °C (a), at 180 °C (b), at 200 °C (c) and at 210 °C (d). Symbols: Experimental data; solid lines: Calculated curves.

Finally, the capability of the model to describe the competition between network structuring and breaking has been tested. Different calculated data have been generated in order to cover a large range of W_i and analyze the competition between structuring and destruction predicted by the model. The results are displayed in Figure 8 where it can be observed that, for large W_i, (W_i = 24 and W_i = 6.5) all data merge to the same limiting Hencky strain. Those results are in pretty good agreement with the experimental results. Indeed, it has been observed that, above a given W_i value, all the conductivity curves merge to the same Hencky strain before conductive/insulating transition (here approximately 1.25 vol%). With the decrease of W_i, the material can undergo larger deformation before becoming electrically insulating (from W_i = 1). This transition from large to low W_i can be well observed in Figure 8.

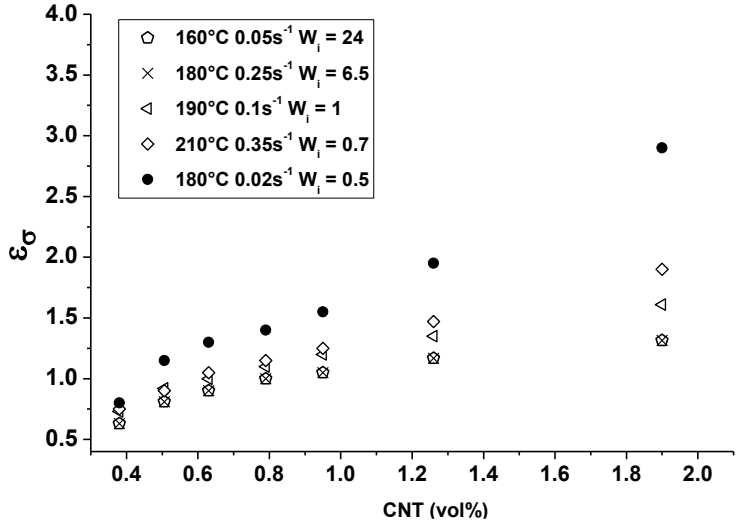

Figure 8: Model prediction of the maximal Hencky strain before conductive/insulating transition for different W_i values.

5. Conclusion

In this work, a new model for the description of the conductivity variation of Conductive Polymer Composites under extensional deformation has been proposed and tested for large ranges of CNTs concentrations and extensional rates. First of all, the proposed model gives the possibility to describe the conductive to insulating transition for experimental conditions that cover a large range of W_i values. Indeed, it well describes the conductivity variation when the destruction is predominant but also when there is a strong competition between structuring and destruction of the network. We have also observed that the structuring mechanism only depends on the temperature and, more precisely, it is directly linked to the weight average relaxation time of the pure matrix. This means that the effect of the temperature on the building parameter can be determined using the Williams Landel Ferry equation applied to the polymer matrix. Hence, the temperature effect is solely in the structuring mechanism. Moreover, the breaking mechanism has been considered directly dependent of the deformation and it turned out that it was independent of the temperature and of the extensional rate. In some cases, the model overestimates the limit of the

material. It occurs when the structuring parameter is quite large. After large deformation, the network structuring cannot be considered anymore as efficient as it would for an isotropic filler network.

This model presents a large domain of validity and gives the possibility to predict the limit of the composite under extensional deformation. We assume that the building and breaking parameters are linked to the type of CNTs and the dispersion state of the CNTs within the polymer matrix. In addition, this model can be extended to different kinds of composites. For example, it can be successfully applied to specimens made of High Impact Polystyrene matrix filled with CNT. Moreover, the model might be generalized to take into account other types of deformation such as planar flow or even shear.

Acknowledgements

This work was funded by the French National Association for Research and Technology and the company Total (CIFRE convention N°2014/0672). The authors kindly thank doctor G. Seytre and technician L. Cavetier for helping setting-up the home made EVF system and engineer and laboratory technician Eddi Scandino for the generation of the different composites.

References:

[1] S. Kirkpatrick, Percolation and conduction, Rev. Mod. Phys. 45 (1973) 574–588.

[2] W. Bauhofer, J.Z. Kovacs, A review and analysis of electrical percolation in carbon nanotube polymer composites, Compos. Sci. Technol. 69 (2009) 1486–1498.

[3] H. Pang, L. Xu, D.X. Yan, Z.M. Li, Conductive polymer composites with segregated structures, Prog. Polym. Sci. 39 (2014) 1908–1933.

[4] T. McNally, P. Pötschke, Polymer-carbon nanotube composites: Preparation, Properties and Applications, Woodhead Publishing Limited, 2011; Part I, pp 92-152.

[5] I. Alig, P. Pötschke, D. Lellinger, T. Skipa, S. Pegel, G.R. Kasaliwal, T. Villmow, Establishment, morphology and properties of carbon nanotube networks in polymer melts, Polymer 53 (2012) 4-28.

[6] L. Moreira, R. Fulchiron, G. Seytre, P. Dubois, P. Cassagnau, Aggregation of Carbon Nanotubes in Semi-dilute Suspension, Macromolecules 43 (2010) 1467-1472.

[7] S. Pegel, P. Pötschke, G. Petzold, I. Alig, S.M. Dudkin, D. Lellinger, Dispersion, agglomeration, and network formation of multiwalled carbon nanotubes in polycarbonate melts, Polymer 49 (2008) 974–984.

[8] J. Obrzut, J.F. Douglas, S.B. Kharchenko, K.B. Migler, Shear-induced conductor–insulator transition in melt-mixed polypropylene–carbon nanotube dispersions, Phys. Rev. B 76 (2007) 195420 /1-9.

[9] S.B. Kharchenko, J.F. Douglas,J. Obrzut, E.A. Grulke, K.B. Migler, Flow-induced properties of nanotube-filled polymer materials, Nat. Mater. 3 (2004) 564–568.

[10] C.A. Martin, J.K. Sandler, W. Shaffer, M.S.P. Schwarz, W.M.K. Bauhofer, K. Schulte, A.H. Windle, Formation of percolating networks in multi-wall carbon nanotube epoxy composites, Compos. Sci. Technol. 64 (2004) 2309–2316.

[11] A.W.K. Ma, M.R. Mackley, S.S. Rahatekar, Experimental observation on the flow-induced assembly of carbon nanotube suspensions to form helical bands, Rheol. Acta 46 (2007) 979-987.

[12] J.K.W. Sandler,A.H. Windle, C.A. Martin, M.L. Schwarz, W. Bauhofer, K. Schulte, M.S.P. Shaffer, Percolation in multi-wall carbon nanotube-epoxy composites: influence of processing parameters, nanotube aspect ratio and electric fields on the bulk conductivity, Mater. Res. Soc. Symp. Proc. 788 (2004) 221–226.

[13] J.Z. Kovacs; B.S. Velagala, K. Schulte, W. Bauhofer, Two percolation thresholds in carbon nanotube epoxy composites, Compos. Sci. Technol. 67 (2007) 922–928.

[14] I. Alig, D. Lellinger, S.M. Dudkin, P. Pötschke, Conductivity spectroscopy on melt processed polypropylene multiwalled carbon nanotube composites: Recovery after shear and crystallization, Polymer 48 (2007) 1020-1029.

[15] W. Bauhofer, S.C. Schulz, A.E. Eken, T. Skipa, D. Lellinger, I. Alig, E.J. Tozzi, D.J. Klingenberg, Shear-controlled electrical conductivity of carbon nanotubes network suspended in low and high molecular weight liquids, Polymer 51 (2010) 5024-5027.

[16] T. Villmow, S. Pegel, P. Pötschke, U. Wagenknech, Influence of injection molding parameters on the electrical resistivity of polycarbonate filled with multiwalled carbon nanotubes, Compos. Sci. Technol., 68 (2008) 777–789.

[17] M. Marcourt, R. Fulchiron, P. Cassagnau, D. Rousseau, O. Lhost, S. Karam, An original combined method for electrical conductivity measurement of polymer composites under extensional deformation, J. Rheol. 2017 61 (2017) 845-851.

[18] T. Skipa, D. Lellinger, M. Saphiannikova, I. Alig, Shear-stimulated formation of carbon nanotube networks in polymer melts, Phys. Status Solidi B 246 (2009) 2453–2456.

[19] T. Skipa, D. Lellinger, W. Böhm, M. Saphiannikova, I. Alig, Influence of shear deformation on carbon nanotube networks in polycarbonate melts: interplay between build-up and destruction of agglomerates, Polymer 51 (2010) 201–210.

[20] H. Barnes, Thixotropy a review, J. Non-Newton. Fluid Mech. 70 (1997), 1-33.

[21] M. Chen, W.B. Russel, Characteristic of flocculated silica dispersion, J. Colloid Interface Sci. 141 (1991) 564-577.

[22] P. Coussot, A.I. Leonov, J.-M.Piau, Rheology of concentrated dispersal systems in a low molecular weight matrix, J. Non-Newton. Fluid Mech. 46 (1993) 94-114.

[23] D. De Kee, R. Code, G. Turcotte, Flow properties of time dependent food stuffs, J. Rheol. 27 (1983) 581-604.

[24] D. Quemada, Rheology of concentrated dispersed systems and minimum energy dissipation principle. I Viscosity-concentration relationship, Rheol. Acta 16 (1977) 82-94.

[25] F. Yziquel, P.J.Carreau, P.A. Tanguyn, Non-linear viscoelastic behavior of fumed silica suspensions, Rheol. Acta 38 (1999) 14-25.

[26] A.I. Leonov, On the rheology of filled polymers, J. Rheol. 34 (1990) 1039-1068.

[27] I.Alig, T. Skipa, D. Lellinger, P. Pötschke, Destruction and formation of a carbon nanotube network in polymer melts: Rheology and conductivity spectroscopy, Polymer 49 (2008) 3524-3532.

[28] Y.Y.S. Huang, E.M. Terentjev, Dispersion of Carbon Nanotubes: Mixing, Sonication, Stabilization and Composite Properties, Polymers 4 (2012) 275-295.

[29] E. Chang, A. Ameli, L.H. Mark, C.B. Park, Effects of uniaxial and biaxial orientation on fiber percolation in conductive polymer composites, AIP Conf. Proc. 1695 (2015) 020027

[30] F. Du, J. Fischer, K. Winey, Effect of nanotube alignment on percolation conductivity in carbon nanotube/polymer composites, Phys. Rev. B 72 (2005) 121404/1-5

[31] R.B. Bird, R.C. Armstrong, O.Hassager, Dynamics of polymeric liquids. Vol. 1, Fluid mechanics, John Wiley & Sons, New York, 1987, pp. 784-785.

[32] J.D. Ferry, Viscoelastic properties of polymers, third ed., John Wiley & Sons, New-York, 1980.

List of figures and tables